

# Impact of environmental moisture on tropical cyclone intensification

Longtao Wu<sup>1,2</sup>, Hui Su<sup>1</sup>, Robert G. Fovell<sup>3</sup>, Timothy J. Dunkerton<sup>4</sup>, Zhuo Wang<sup>5</sup>,  
and Brian H. Kahn<sup>1</sup>

*1. Jet Propulsion Laboratory, California Institute of Technology, Pasadena, California*

*2. Joint Institute for Regional Earth System Science and Engineering, University of  
California, Los Angeles, California*

*3. University of California, Los Angeles, Los Angeles, California*

*4. Northwest Research Associates, Inc., Bellevue, Washington*

*5. University of Illinois at Urbana-Champaign, Urbana, Illinois*

Submitted to *Atmospheric Chemistry and Physics*

September, 2015

Copyright: © 2015 California Institute of Technology.  
All rights reserved.

---

*Corresponding author address:* Longtao Wu, 4800 Oak Grove Dr., M/S 183-701, Pasadena, CA  
91109  
E-mail: Longtao.Wu@jpl.nasa.gov

## 33 **Abstract**

34       The impacts of environmental moisture on the intensification of a tropical cyclone (TC) are  
35 investigated in the Weather Research and Forecasting (WRF) model, with a focus on the  
36 azimuthal asymmetry of the moisture impacts relative to the storm path. A series of sensitivity  
37 experiments with varying moisture perturbations in the environment are conducted and the  
38 Marsupial Paradigm framework is employed to understand the different moisture impacts. We  
39 find that modification of environmental moisture has insignificant impacts on the storm in this  
40 case unless it leads to convective activity that deforms the quasi-Lagrangian boundary of the  
41 storm and changes the moisture transport into the storm. By facilitating convection and  
42 precipitation outside the storm, enhanced environmental moisture ahead of the northwestward-  
43 moving storm induces a dry air intrusion to the inner core and limits TC intensification. In  
44 contrast, increased moisture in the rear quadrants favors intensification by providing more  
45 moisture to the inner core and promoting storm symmetry, with primary contributions coming  
46 from moisture increase in the boundary layer. The different impacts of environmental moisture  
47 on TC intensification are governed by the relative locations of moisture perturbations and their  
48 interactions with the storm Lagrangian structure.

49

## 50 **1. Introduction**

51 While the forecast of tropical cyclone (TC) tracks has been significantly improved in the  
52 past several decades, the TC intensity forecast is still a great challenge for most operational  
53 numerical weather prediction (NWP) centers (DeMaria et al. 2007). Environmental moisture has  
54 been considered as one of the important factors for TC intensity forecasting. As one of the  
55 skillful predictors, the 850 hPa relative humidity (RH) averaged between 200 km and 800 km  
56 from storm center has been used routinely in the Statistical Hurricane Intensity Prediction  
57 Scheme (SHIPS) for hurricane intensity forecast in the National Hurricane Center (NHC)  
58 (Kaplan et al. 2010).

59 Theoretical and modeling studies have suggested high environmental moisture may be  
60 conducive to TC intensification (e.g., Emanuel et al. 2004; Kimball 2006). Dry air intrusion  
61 could lead to a weakening of a TC by inducing asymmetric convective activity and/or  
62 transporting low equivalent potential temperature ( $\theta_e$ ) air into the sub-cloud layer and storm  
63 inflow (e.g., Braun et al. 2012; Emanuel 1989; Ge et al. 2013; Kimball 2006; Tao and Zhang  
64 2014). However, some studies (e.g., Kimball 2006; Wang 2009; Ying and Zhang 2012) showed  
65 that substantial moisture may also cause a negative impact on TC strength by facilitating the  
66 formation of TC rainbands, which reduces the horizontal pressure gradient of a TC. In idealized  
67 simulations, Hill and Lackmann (2009) varied RH values in the moist envelope 100 km beyond  
68 the TC core and found that larger RH results in the establishment of wider TCs with more  
69 prominent outer rainbands. However, in their study, TC intensity was nearly insensitive to  
70 environmental RH despite the variation in rainband activity.

71 Braun et al. (2012) showed that dry air located 270 km away from the storm center had  
72 little impact on hurricane intensity with no mean flow. Dry air intrusion into the storm vortex,

73 however, suppressed convective activity and increased the asymmetry of convection, leading to a  
74 weakening of the storm. While a dry air envelope had no significant impact on hurricane  
75 intensity, the storm size was reduced. Vertical shear can significantly enhance the suppression  
76 effect of dry air intrusion (Tang and Emanuel 2012; Ge et al. 2013; Tao and Zhang 2014). By  
77 modifying the diabatic heating rate due to cloud microphysical process, Wang (2009)  
78 demonstrated that diabatic cooling in the outer spiral rainbands helped the TC remain intense and  
79 compact. Increased latent heat release in the outer spiral rainbands decreased the intensity but  
80 increased the TC size. In a sensitivity study of Typhoon Talim (2005), Ying and Zhang (2012)  
81 showed that enhanced moisture promoted convection in outer rainbands and resulted in the  
82 weakening of the storm while dry air inhibited outer rainbands and contributed to a stronger  
83 storm with smaller size. The storm was more sensitive to the moisture perturbation residing to  
84 the north than to the south due to its shorter travel time into the storm vortex.

85 Composite studies using analyses datasets and satellite observations (Kaplan and  
86 DeMaria 2003; Hendricks et al. 2010; Wu et al. 2012) have shown that rapid intensification (RI)  
87 of TCs is associated with higher environmental RH in the lower and middle troposphere than  
88 non-RI events. Using satellite observations, Shu and Wu (2009) showed that the dry Saharan air  
89 layer (SAL) can affect TC intensity in both favorable and unfavorable manners. TCs tend to  
90 intensify when dry SAL air is present in the northwest quadrant of TCs. However, TCs tend to  
91 weaken when dry air intrudes within 360 km of the TC center in the southwest and southeast  
92 quadrants. Substantial azimuthal asymmetry of RH is also found in TCs' environment based on  
93 nine years of satellite observations, with rear quadrants (relative to storm motion) being moister  
94 than front quadrants, especially during RI (Wu et al. 2012).

95           Most previous modeling studies prescribed moisture perturbations without specifically  
96 considering their relative location to a storm vortex (e.g., in the environment, outer rainband or  
97 inner core; front or rear quadrants), which may cause different impacts on the storm structure and  
98 intensity. In this study, we investigate the impacts of environmental moisture on TC intensity and  
99 structure using the Weather Research and Forecasting (WRF) model with artificially modified  
100 environmental moisture surrounding a storm vortex. Guided by the observational composite  
101 study by Wu et al. (2012), we focus on the azimuthally asymmetric effects of environmental  
102 moisture in the front and rear quadrants. Section 2 provides the model description and  
103 experiment design. The Marsupial Paradigm framework (Dunkerton et al. 2009) is also  
104 introduced in section 2 as a tool to interpret the moisture impacts on the storm. Section 3  
105 describes the evolution of the simulated storm in the control experiment. The results from  
106 sensitivity experiments are presented in section 4. The findings from this study are summarized  
107 in section 5.

## 108 **2. WRF experiments and analysis framework**

### 109 *a. Model description*

110           To examine the role of environmental moisture on TC intensification, we drive the WRF  
111 model with initial and boundary conditions from a real-case hurricane, in particular, Hurricane  
112 Earl (2010). Hurricane Earl originated from a tropical wave west of the Cape Verde Islands on  
113 23 August 2010. It moved westward across the Atlantic and gradually strengthened to a tropical  
114 storm. Before the RI at 0000 UTC 29 August (Fig. 1a), a dry zone consisting of precipitable  
115 water vapor (PWV) less than 4.5 cm was located to the west of the storm, in the front quadrant  
116 relative to the storm propagation. Meanwhile, a broad moist region was observed to the south  
117 and southeast of the storm. Such a “dry front and moist rear” environmental moisture structure is

118 typical of a rapidly intensifying hurricane as found in Wu et al. (2012). Earl underwent a RI from  
119 0600 UTC 29 August to 0000 UTC 31 August. The maximum wind speed (MWSP) increased by  
120  $31 \text{ m s}^{-1}$  while the minimum sea level pressure (MSLP) deepened by 53 hPa in 36 h.

121 Inspired by the rapid intensification of Hurricane Earl (2010), we initialize the Advanced  
122 Research WRF model V3.3.1 (Skamarock et al. 2008) at 0000 UTC 29 August, 2010 and run it  
123 for 48 h. Simulations are conducted with a parent grid at 9 km horizontal resolution and a vortex-  
124 following nested grid at 3 km resolution. Experiments show that simulated results are not  
125 sensitive to the horizontal resolution of the parent grid with similar inner domains. There are 50  
126 model levels in the vertical from the surface to 20 hPa, and the initial and boundary conditions  
127 were derived from the interim ECMWF (European Centre for Medium-Range Weather  
128 Forecasts) reanalysis (ERA-Interim) (<http://rda.ucar.edu/datasets/ds627.0/>). For all the  
129 experiments, we employ the Thompson et al. (2008) microphysical scheme, the Rapid Radiative  
130 Transfer Model for GCMs (RRTMG) shortwave and longwave schemes (Iacono et al. 2008), and  
131 the Yonsei University planetary boundary layer (PBL) scheme (Hong et al. 2006). The Kain-  
132 Fritsch cumulus scheme (Kain 2004) is used in the parent domain while no cumulus scheme is  
133 used in the moving nested inner grids.

134 As the model is initialized solely from the coarse-resolution reanalysis, the initial TC is  
135 weaker and less organized than the actual storm was and thus at least a portion of its subsequent  
136 intensification represents a response to the improved resolution. *Our focus is on how*  
137 *environmental moisture perturbations directly and indirectly influence how the storm organizes*  
138 *subsequent to initialization.* To assess potential impacts of the initial conditions, the WRF  
139 control (CTRL) simulation consists of five ensemble members with randomly generated RH  
140 perturbations of less than 1% added to the initial specific humidity field at all model horizontal

141 and vertical grids. In the following discussions, the CTRL and other sensitivity experiments refer  
142 to the ensemble means of the respective five ensemble members.

### 143 ***b. Experiment design***

144 The sensitivity experiments are conducted by placing moisture perturbations of varying  
145 magnitudes at different locations relative to the storm at the initial time (Fig. 1). The zones are  
146 rectangular in shape and sharply bounded and, as a consequence, could serve as focal points for  
147 convective activity if conditions are sufficiently favorable. We explored tapering the edges of  
148 the moisture perturbations and found it did not materially alter our conclusions.

149 In the Moist Front (MF) experiment (Fig. 1b), an artificially moistened zone of 5 degrees  
150 in longitude and 7 degrees in latitude is placed in front of the storm (relative to its roughly  
151 westward propagation). Within the moist zone, the RH of all model grids from 900 hPa to the  
152 model top of 20 hPa are set to the maximum RH within the outer radius of the storm at each level  
153 by modifying specific humidity without changing temperature. In the Intermediate Moist Front  
154 (MFI) simulation (Fig. 1c), the moist zone is located at the same place as for MF but the  
155 magnitude of the moisture perturbation is smaller (70% of the maximum RH at each level).  
156 Thus, the CTRL, MFI and MF cases represent the dry, intermediate moist and moist  
157 environments at the front of the storm, respectively.

158 In the Moist Rear (MR) simulation, a moist zone with the same area and magnitude of  
159 RH perturbations as in the MF run is placed to the south, roughly in the storm's rear quadrants  
160 (Fig. 1d). The Dry Rear (DR) simulation (Fig. 1e) is similar to the MR simulation but the  
161 magnitude of the RH perturbation is reduced to 30% of the maximum RH at each level, which is  
162 drier than the CTRL. So the dry, intermediate moist and moist environments at the rear of the  
163 storm are represented by the DR, CTRL and MR experiments, respectively.

164 Further sensitivity experiments with moisture zones of different sizes were also tested,  
165 and the results are not qualitatively sensitive to the choice of the areal extent of the moist zone.  
166 For brevity, only MF, MFI, MR and DR are discussed in addition to the CTRL. We also perform  
167 a set of simulations in which the vertical extent of the moisture perturbations in the MR  
168 configuration is varied to examine the vertical dependence of the environmental moisture  
169 impacts.

### 170 *c. Marsupial Paradigm*

171 The Marsupial Paradigm is a framework proposed by Dunkerton et al. (2009) to study the  
172 formation of a TC within tropical waves. Dunkerton et al. (2009) demonstrated that the critical  
173 layer of a tropical easterly wave is a region of approximately closed Lagrangian circulation (also  
174 called a “wave pouch”). The wave pouch protects the TC vortex from dry air intrusion to some  
175 extent, rendering a favorable environment for deep convection and TC formation. Owing to  
176 convergent flow, the wave pouch may have an opening that allows the influx of environmental  
177 air (see Figure 3 in Wang et al. 2010). The Lagrangian boundary of the storm and its interaction  
178 with the ambient environment can be clearly illustrated by the streamlines in a frame of reference  
179 moving at the same speed with the wave (Fritz and Wang 2013; Montgomery et al. 2010; Wang  
180 et al. 2009; 2012a; 2012b). The translated streamlines in a co-moving frame, which resemble the  
181 flow trajectories, provide a Lagrangian view of the storm evolution. Although the Marsupial  
182 Paradigm framework was proposed for TC formation, we adopt the concept in this study to  
183 investigate the impacts of asymmetric environmental moisture on TC intensification and  
184 structure. In the following analysis, the modeled streamlines are translated from the Earth-  
185 relative frame to the co-moving frame based on the estimated storm propagation speed from the  
186 automatic vortex-following algorithm in the WRF.



### 187 3. Storm evolution in the control simulation

188 As shown in Fig. 2, the simulated storm in the CTRL experiment (red lines) intensifies in  
189 the first 24 h. During 24-30h, the simulated MSLP shows a slowing down of the intensification  
190 (Fig. 2a) while the MWSP (Fig. 2b) exhibits a weakening trend. The storm continues its  
191 intensification in the following 18 h. The MWSP of the simulated storm increases by  $21 \text{ m s}^{-1}$   
192 from 6-h to 48-h while the MSLP deepens by 38 hPa. The simulated intensification rate in the  
193 CTRL experiment is less than that for Hurricane Earl (2010). Since this study focuses on  
194 understanding the role of environmental moisture in TC intensification, the differences between  
195 the sensitivity experiments and the CTRL are of interest. The difference between the simulated  
196 storm in the CTRL experiment and observed Hurricane Earl is not a primary concern.

197 Figure 3 shows the PWV and translated streamlines of the WRF CTRL simulation in the  
198 co-moving frame. Averages over four periods (0-6 h, 12-18 h, 30-36 h and 42-48 h) are  
199 displayed. At the initial time (Fig. 3a), the storm core (indicated by the relative large  $\text{PWV} > 5$   
200 cm) is collocated with the storm Lagrangian structure (indicated by the nearly enclosed  
201 streamlines). The storm Lagrangian structure is closed to the west of the storm, where dry air is  
202 located. Thus, there is a favorable environment for the intensification of the storm, as dry air  
203 intrusion would be limited and moisture in the vortex can be preserved. The inner region of the  
204 storm continues to moisten (Fig. 3b) as the storm intensifies in the first 24 h (Fig. 2), and the dry  
205 zone to the northwest of the storm becomes even drier (Fig. 3b). On the other hand, the moist  
206 region to the south and southeast of the storm diminishes in magnitude. The storm Lagrangian  
207 structure is open to the southwest at this time. In the next 24 h (Fig. 3c and 3d), the storm center  
208 keeps moistening while the dry air approaches the opening of the storm Lagrangian structure to  
209 the southwest of the storm.

## 210 **4. Impacts of Environmental Moisture**

### 211 *a. Summary of sensitivities in TC intensity and track*

212 Figure 2a shows the evolution of MSLP from four sensitivity experiments for comparison  
213 with the CTRL simulation. Except for the first 6 h of the 48-h integration, the MF experiment  
214 (with an ensemble mean of 990 hPa at the 24-h simulation) has higher MSLP than the CTRL  
215 simulation (whose ensemble mean is 967 hPa at that same time). The MR experiment produces  
216 comparable (or slightly higher) MSLP to the CTRL simulation in the first 24 h. Afterwards, the  
217 storm in the MR experiment strengthens much faster than its CTRL counterpart. The MSLP in  
218 the MR simulation reaches 953 hPa at the 48-h forecast, the lowest among all the experiments.  
219 Similar experiments with initialization at 12 hours earlier show consistent results to the CTRL,  
220 MF and MR experiments, except a more intense storm developed in the experiment with a moist  
221 perturbation in the rear (figure not shown). Both the MFI and DR simulations have minor  
222 impacts on hurricane intensity, compared to the CTRL, throughout the 48-h integration.

223 Similar trends of storm evolution appear in the simulated MWSP (Fig. 2b). Both the MF  
224 and MR simulations produce a stronger storm at the 6-h forecast than the CTRL run. Between 18  
225 h and 24 h, the strength of the storm is comparable between MF and MR, but weaker than that in  
226 the CTRL. After 30 h, the MF experiment produces a weaker storm relative to the CTRL  
227 simulation while the storm intensifies faster in the MR run. By the end of the simulation at 48 h,  
228 the ensemble mean MWSP is  $35 \text{ m s}^{-1}$  for MF,  $43 \text{ m s}^{-1}$  for CTRL, and  $50 \text{ m s}^{-1}$  for MR.  
229 Consistent with MSLP, both the MFI and DR experiments have no significant impacts on the  
230 magnitude of MWSP relative to the CTRL.

231 Regarding storm track (Fig. 4), the storm in the MF experiment moves further  
232 northwestward than the CTRL case. A significant track difference starts to show at 12 h,

233 corresponding to the change in the MSLP. In the first 24 h, the track differences are less than 110  
234 km. When the storm executes a gradual curve to the northwest, the track differences increase  
235 with a maximum difference of 220 km at 48 h. In the last 24 h, the significant deflection to the  
236 north with lower SST may partly contribute to the weaker storm in the MF experiment. The MR  
237 experiment has relatively small changes on the storm track. In the last 24 h, the storm in the MR  
238 experiment moves less northward comparing to the storm in the CTRL experiment, along with  
239 stronger intensification in the MR. The track differences are less than 70 km between MR and  
240 CTRL for all the 48-h integration. The track differences from the CTRL experiment are  
241 insignificant in the MFI and DR experiments (not shown).

242 Details of the storm evolution in each sensitivity experiment are investigated in a storm-  
243 following framework in the following subsections.

#### 244 ***b. MF experiment***

245 Figure 5 shows the differences of PWV and winds between the MF and CTRL  
246 experiments. At the initialization of the simulation (Fig. 5a), a nearly saturated region with a  
247 large amount of water vapor is prescribed to the west of the storm, where it is dry in the CTRL.  
248 The prescribed moist zone is outside of the storm Lagrangian boundary. In the following 18 h,  
249 extensive precipitation (maximized between 6-12 h; not shown) develops within the prescribed  
250 moist zone in the MF experiment (Fig. 6b), which is absent in the CTRL simulation (Fig. 6a).  
251 This supplemental convective activity induces a cyclonic circulation around the prescribed moist  
252 zone in the environment of the storm, resulting in a deformation of the storm Lagrangian  
253 structure with divergence to the west of the storm center (Fig. 5b).

254 Consequently, both moist air from the prescribed moist zone and dry air in the  
255 environment intrude into the storm vortex from the convective-deformed portion, leading to an

256 asymmetric moisture structure (Fig. 5b-5d) and diabatic heating fields (Fig. 6b and 7). Dry  
257 environmental air has reached the storm inner core at 30-36 h (Fig. 5c). At 42-48 h forecast, a  
258 spiral band of convection with closed ring in the inner core forms in the CTRL case (Fig. 7d)  
259 while only a comma shape of convection is produced in the MF experiment (Fig. 7e) with much  
260 weaker storm intensity (Fig. 7f). In summary, convection in the environment in the MF case  
261 deforms the storm Lagrangian structure towards the dry front-side environment and facilitates  
262 the intrusion of dry air from the north into the inner core, creating asymmetric convection in the  
263 inner core and leading to the weakening of the storm (Nolan and Grasso 2003; Nolan et al.  
264 2007).

### 265 *c. MR experiment*

266 In the MR experiment, the prescribed moist zone is located in the already relatively moist  
267 environment to the south of the storm, outside of the storm Lagrangian boundary (Fig. 8a).  
268 Similar to the MF case, the nearly saturated moist perturbation induces convective activity and  
269 precipitation (Fig. 6c) beyond the storm vortex in the first 18 h, resulting in a weaker storm  
270 compared to the CTRL case prior to 26h (Fig. 2). Different from the MF case, the convection-  
271 induced deformation helps transport moisture to the east portions of the storm without an  
272 accompanying dry air intrusion (Fig. 8b).

273 Therefore, by 30-36 h (Fig. 8c), more moisture appears within the core and also on the  
274 storm's north flank, where it is also moister than in the CTRL case (Fig. 3c). This results in a  
275 more symmetric storm, with better-defined spiral rainbands than the CTRL (Fig. 9a and 9b).  
276 Subsequently, the MR storm starts strengthening faster than the CTRL (Fig. 2 and Fig. 9c), and  
277 by the end of the 48-h integration, the convective activity of the inner core in the MR case (Fig.  
278 9e) shows a nearly concentric ring without the long tail of the spiral band seen in the CTRL case

279 (Fig. 9d). In summary, the convection in the environment enhances the inflow to the storm  
280 Lagrangian structure from the moist region and facilitates the moisture transport into the storm  
281 inner core in the MR case, leading to a more symmetric storm with higher intensity.

#### 282 ***d. MFI and DR experiments***

283 The MFI and DR experiments are similar to the MF and MR cases, respectively, except  
284 that their RH perturbation magnitude at each level is reduced in the prescribed zone. In both of  
285 the MFI and DR experiments (Fig. 10), the moisture perturbations do not promote convective  
286 activity in the environment of the storm. Throughout the 48-h integration, the storms in both the  
287 MFI and DR experiments contain the Lagrangian structures comparable to the CTRL case. The  
288 Lagrangian structure protects the storm well from intrusion of the environmental air. The  
289 prescribed moist air in the MFI and dry air in the DR wrap around the storm without entrainment  
290 into the storm vortex during the 48-h integration. There is no significant change in storm  
291 intensity and vortex structure of the MFI and DR experiments compared to the CTRL simulation.  
292 This is broadly consistent with Braun et al. (2012) that environment moisture content does not  
293 necessarily affect the storm intensity when the perturbation magnitude is not significant.

#### 294 ***e. Height dependency***

295 Another set of experiments are conducted to identify which layer of moisture is more  
296 important to promote TC intensification in the MR experiment. In these simulations, we limit the  
297 vertical extent of the moist perturbation to 900-500 hPa, 900-300 hPa, 850-500 hPa, 500-300  
298 hPa, 500-20 hPa, and 300-20 hPa, respectively. It is found that only the RH enhancements  
299 including the boundary layer (900-300 hPa and 900-500 hPa cases) promote significant  
300 intensification of the storm relative to the CTRL simulation (Fig. 11). When extra moisture is  
301 provided above 850 hPa, the intensity of the storm is quite similar to the CTRL run or even

302 slightly weaker than the CTRL case by the end of the simulations at 48-h integration, although  
303 convective activity induced by moisture perturbation is produced outside of the storm in some  
304 cases (for example, the 850-500 case). Note that saturation water vapor content in the boundary  
305 layer is significantly higher than in the middle and upper troposphere. Therefore, a small increase  
306 of RH in the boundary layer can provide much more moist static energy to fuel the storm  
307 intensification.

## 308 **5. Summary and Discussion**

309 The impacts of environmental moisture on TC intensity are examined in the WRF model,  
310 with a focus on the azimuthal asymmetry of moisture impacts. The Marsupial Paradigm  
311 framework is used to understand the evolution of the storm. The intensification process of a  
312 storm is simulated in the WRF CTRL simulation. When the moisture perturbation is not large  
313 enough to create additional convection outside of the storm, as in the MFI and DR experiments,  
314 the storm Lagrangian boundary serves as a barrier to protect the storm from intrusion of  
315 environmental air. No significant impact on the storm intensity and track is observed in the MFI  
316 and DR experiments.

317 However, when convective activity is promoted by the moisture perturbation and deforms  
318 the storm Lagrangian structure, as in the MF experiment, a storm that is weaker than the CTRL  
319 case occurs due to intrusion of dry environmental air from the northwest into the vortex through  
320 the convective-induced open Lagrangian structure, which leads to the asymmetry of convection  
321 in the storm inner core. The storm is also deflected to further northwest and approaches dry air,  
322 especially in the last 24 h, which may also contribute to the weaker storm in the MF experiment.  
323 In contrast, convective deformation of the vortex in the MR experiment facilitates the  
324 entrainment of additional moisture from the south and results in more symmetric and powerful

325 convection in the inner core with a higher intensity than the CTRL case. The intensification is  
326 primarily contributed by enhanced moisture in the boundary layer. The distortion of the storm  
327 Lagrangian structure and changes in the moisture pathway play the key roles in the different  
328 response of the MF and MR cases.

329         This study demonstrates that the Marsupial Paradigm is a useful tool to study the  
330 interaction of a TC vortex with its environment at any stage of the storm development, not only  
331 limited to TC formation. Dunkerton et al. (2009) proposed that a closed circulation is favorable  
332 for TC formation. This study hypothesized an open storm Lagrangian structure can also benefit  
333 TC formation and intensification as long as the opening is towards a favorable environment (e.g.,  
334 moist air).

335         Based on these results and previous studies (Braun et al. 2012; Ge et al. 2013; Hill and  
336 Lackmann 2009; Kimball 2006; Tao and Zhang 2014; Wang 2009; Ying and Zhang 2012), we  
337 conclude that environmental moisture has limited impacts on storm intensity if it does not enter  
338 the storm vortex, similar to the insignificant impacts of dry air beyond 270 km noted in Braun et  
339 al. (2012). If the moisture enhancement produces enhanced convective activity within the vortex,  
340 however, the direct and indirect impacts on the storm can be complex. By itself, enhanced outer  
341 rainband activity (the direct effect) may weaken the storm (Wang 2009; Ying and Zhang 2012).  
342 Yet, the convective activity could also deform the storm vortex, more indirectly leading to  
343 changes in the nature of the moisture inflow. Consistent with conventional understanding, a dry  
344 air intrusion into the inner core that might opportunistically cause a vortex deformation (as in the  
345 MF case) and suppress the storm, while an enhanced moisture supply into the inner core (as in  
346 the MR case) promotes intensification of the storm. The disparate responses of TC intensity to  
347 moisture perturbations in the literature may largely be a result of the different magnitudes and

348 relative locations of moisture perturbations to the storm vortex, and thus their different abilities  
349 to deform the storm vortex.

350         This study demonstrates that storm structure is critical for understanding environmental  
351 impacts on TCs. Previous composite data analyses have been sampled with respect to the  
352 distance from the storm center, without consideration on the storm (structure). Most modeling  
353 studies prescribed moisture perturbations, but did not pay much attention to their relative  
354 locations to the storm vortex. As shown in this study and previous papers, TCs respond  
355 differently to moisture perturbations in different locations (the inner core, the outer rainband  
356 region and the more distant environment). Thus, in order to better quantify moisture impacts on  
357 TCs, it is necessary to distinguish moisture in the outer rainband and moisture in the inner core  
358 of the storm as well as different environmental moisture distributions.

359         This study also explains, to some degree, the observational results by Shu and Wu (2006)  
360 that the dry SAL may have favorable or unfavorable impacts on TC intensification, depending on  
361 its position. Considering that the TCs in the North Atlantic usually have moisture inflow from  
362 the southern quadrants, when the SAL is located to the northwest of TCs, it may not affect the  
363 storm intensity, or may even indirectly favor TC intensification by suppressing the formation of  
364 convective rainbands outside of the storm. When dry air is located to the southeast or southwest  
365 of the TCs, however, the dry air may be entrained into the storm, leading to a weakening effect.  
366 The MF and MR experiments suggest that the “dry front and moist rear” distribution of  
367 environmental moisture is a favorable condition for TC intensification, consistent with the  
368 observational study of Wu et al. (2012). Given that environmental moisture can have different  
369 impacts on TCs once it enters into the storm, accurate characterizations of environmental  
370 moisture are important to TC intensity forecasts.



371 This study shows that convection in the environment can have either favorable or  
372 unfavorable impacts on the storm intensity. Thus, a better understanding of the interaction of the  
373 storm with environmental convective activity (e.g. trough interaction with storm) is also critical  
374 to improving TC intensity forecasts.

### 375 **Acknowledgements**

376 The work is conducted at the Jet Propulsion Laboratory, California Institute of Technology,  
377 under contract with NASA. The authors thank the funding support from the NASA Hurricane  
378 Science Research Program. Wang was supported by National Science Foundation Grant AGS-  
379 1118429. Helpful comments from Mark Boothe and Shuyi Chen are appreciated.

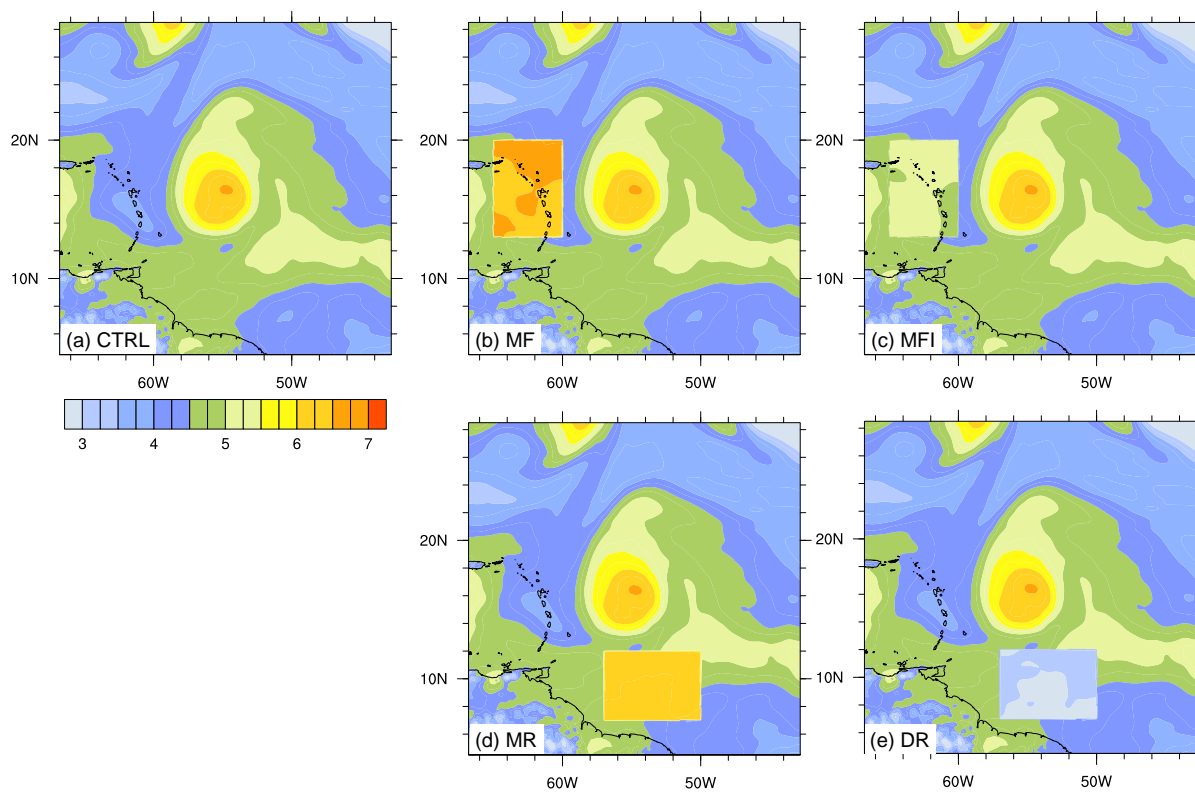
### 380 **References**

- 381 Braun, S. A., J. A. Sippel, D. S. Nolan, 2012: The Impact of Dry Midlevel Air on Hurricane  
382 Intensity in Idealized Simulations with No Mean Flow. *J. Atmos. Sci.*, 69, 236–257. doi:  
383 <http://dx.doi.org/10.1175/JAS-D-10-05007.1>
- 384 DeMaria, M., J. A. Knaff, and C. Sampson, 2007: Evaluation of long-term trends in tropical  
385 cyclone intensity forecasts. *Meteor. Atmos. Phys.*, 97, 19–28.
- 386 Dunkerton, T. J., M. T. Montgomery, and Z. Wang, 2009: Tropical cyclogenesis in a tropical wave  
387 critical layer: Easterly waves. *Atmos. Chem. Phys.*, 9, 5587–5646.
- 388 Emanuel, K.A., 1989: Dynamical theories of tropical convection. *Aust. Meteor. Mag.*, 37, 3-10.
- 389 Emanuel, K., C. DesAutels, C. Holloway and R. Korty, 2004: Environmental control of tropical  
390 cyclone intensity. *J. Atmos. Sci.*, 61, 843–858. doi: [http://dx.doi.org/10.1175/1520-](http://dx.doi.org/10.1175/1520-0469(2004)061<0843:ECOTCI>2.0.CO;2)  
391 [0469\(2004\)061<0843:ECOTCI>2.0.CO;2](http://dx.doi.org/10.1175/1520-0469(2004)061<0843:ECOTCI>2.0.CO;2)
- 392 Fritz, C. and Z. Wang, 2013: A Numerical Study of the Impacts of Dry Air on Tropical Cyclone  
393 Formation: A Development Case and a Nondevelopment Case. *J. Atmos. Sci.*, 70, 91–111. doi:  
394 <http://dx.doi.org/10.1175/JAS-D-12-018.1>

- 395 Ge, X., T. Li, and M. Peng, 2013: Effects of Vertical Shears and Midlevel Dry Air on Tropical  
396 Cyclone Developments. *J. Atmos. Sci.*, 70, 3859–3875. doi: [http://dx.doi.org/10.1175/JAS-D-](http://dx.doi.org/10.1175/JAS-D-13-066.1)  
397 13-066.1
- 398 Hendricks, E. A., M. S. Peng, B. Fu and T. Li, 2010: Quantifying Environmental Control on  
399 Tropical Cyclone Intensity Change. *Mon. Wea. Rev.*, 138, 3243–3271. doi:  
400 <http://dx.doi.org/10.1175/2010MWR3185.1>
- 401 Hill, K. A. and G. M. Lackmann, 2009: Influence of Environmental Humidity on Tropical Cyclone  
402 Size. *Mon. Wea. Rev.*, 137, 3294–3315. doi: <http://dx.doi.org/10.1175/2009MWR2679.1>
- 403 Hong, S-Y, Y. Noh and J. Dudhia, 2006: A New Vertical Diffusion Package with an Explicit  
404 Treatment of Entrainment Processes. *Mon. Wea. Rev.*, 134, 2318–2341. doi:  
405 <http://dx.doi.org/10.1175/MWR3199.1>
- 406 Iacono, M. J., J. S. Delamere, E. J. Mlawer, M. W. Shephard, S. A. Clough, and W. D. Collins,  
407 2008: Radiative forcing by long-lived greenhouse gases: Calculations with the AER radiative  
408 transfer models, *J. Geophys. Res.*, 113, D13103, doi:10.1029/2008JD009944.
- 409 Kain, J. S., 2004: The Kain–Fritsch Convective Parameterization: An Update. *J. Appl. Meteor.*,  
410 43, 170–181. doi: [http://dx.doi.org/10.1175/1520-0450\(2004\)043<0170:TKCPAU>2.0.CO;2](http://dx.doi.org/10.1175/1520-0450(2004)043<0170:TKCPAU>2.0.CO;2)
- 411 Kaplan, J., and M. DeMaria, 2003: Large-scale characteristics of rapidly intensifying tropical  
412 cyclones in the North Atlantic basin, *Wea. Forecasting*, 18:6,1093-1108.
- 413 Kaplan, J., M. DeMaria, J. A. Knaff, 2010: A Revised Tropical Cyclone Rapid Intensification  
414 Index for the Atlantic and Eastern North Pacific Basins. *Wea. Forecasting*, 25, 220–241. doi:  
415 <http://dx.doi.org/10.1175/2009WAF2222280.1>
- 416 Kimball, S. K., 2006: A Modeling Study of Hurricane Landfall in a Dry Environment. *Mon. Wea.*  
417 *Rev.*, 134, 1901–1918. doi: <http://dx.doi.org/10.1175/MWR3155.1>
- 418 Montgomery, M. T., Z. Wang, and T. J. Dunkerton, 2010: Coarse, intermediate and high resolution  
419 numerical simulations of the transition of a tropical wave critical layer to a tropical storm.  
420 *Atmos. Chem. Phys.*, 10, 10 803–10 827.
- 421 Nolan, D. S., L. D. Grasso, 2003: Nonhydrostatic, Three-Dimensional Perturbations to Balanced,  
422 Hurricane-Like Vortices. Part II: Symmetric Response and Nonlinear Simulations. *J. Atmos.*

- 423 *Sci.*, 60, 2717–2745. doi: <http://dx.doi.org/10.1175/1520->  
424 0469(2003)060<2717:NTPTBH>2.0.CO;2
- 425 Nolan, D. S., Y. Moon, D. P. Stern, 2007: Tropical Cyclone Intensification from Asymmetric  
426 Convection: Energetics and Efficiency. *J. Atmos. Sci.*, 64, 3377–3405. doi:  
427 <http://dx.doi.org/10.1175/JAS3988.1>
- 428 Skamarock W. C., Klemp J. B., Dudhia J., Gill D. O., Barker D. M., Wang W. and Powers J. G.,  
429 2008: A Description of the Advanced Research WRF Version 3. *NCAR Technical Note TN-*  
430 *468+STR*. 113 pp.
- 431 Shu, S., and L. Wu, 2009: Analysis of the influence of Saharan air layer on tropical cyclone  
432 intensity using AIRS/Aqua data, *Geophys. Res. Lett.*, 36, L09809,  
433 doi:10.1029/2009GL037634.
- 434 Tang, B. and K. Emanuel, 2012: Sensitivity of tropical cyclone intensity to ventilation in an  
435 axisymmetric model. *J. Atmos. Sci.*, 69, 2394–2413.
- 436 Tao D. and F. Zhang, 2014: Effect of environmental shear, sea-surface temperature, and ambient  
437 moisture on the formation and predictability of tropical cyclones: An ensemble-mean  
438 perspective. *J. Adv. Model. Earth Syst.*, 6, 384–404, doi:10.1002/2014MS000314.
- 439 Thompson, G., P. R. Field, R. M. Rasmussen, W. D. Hall, 2008: Explicit Forecasts of Winter  
440 Precipitation Using an Improved Bulk Microphysics Scheme. Part II: Implementation of a New  
441 Snow Parameterization. *Mon. Wea. Rev.*, 136, 5095–5115. doi:  
442 <http://dx.doi.org/10.1175/2008MWR2387.1>
- 443 Wang, Y., 2009: How Do Outer Spiral Rainbands Affect Tropical Cyclone Structure and Intensity?  
444 *J. Atmos. Sci.*, 66, 1250–1273. doi: <http://dx.doi.org/10.1175/2008JAS2737.1>
- 445 Wang, Z., M. T. Montgomery, and T. J. Dunkerton (2009), A dynamically-based method for  
446 forecasting tropical cyclogenesis location in the Atlantic sector using global model products,  
447 *Geophys. Res. Lett.*, 36, L03801, doi:10.1029/2008GL035586.
- 448 Wang, Z., M. T. Montgomery, and T. J. Dunkerton (2010), Genesis of Pre-hurricane Felix (2007).  
449 Part I: The Role of the Wave Critical Layer. *J. Atmos. Sci.*, 67, 1711–1729.

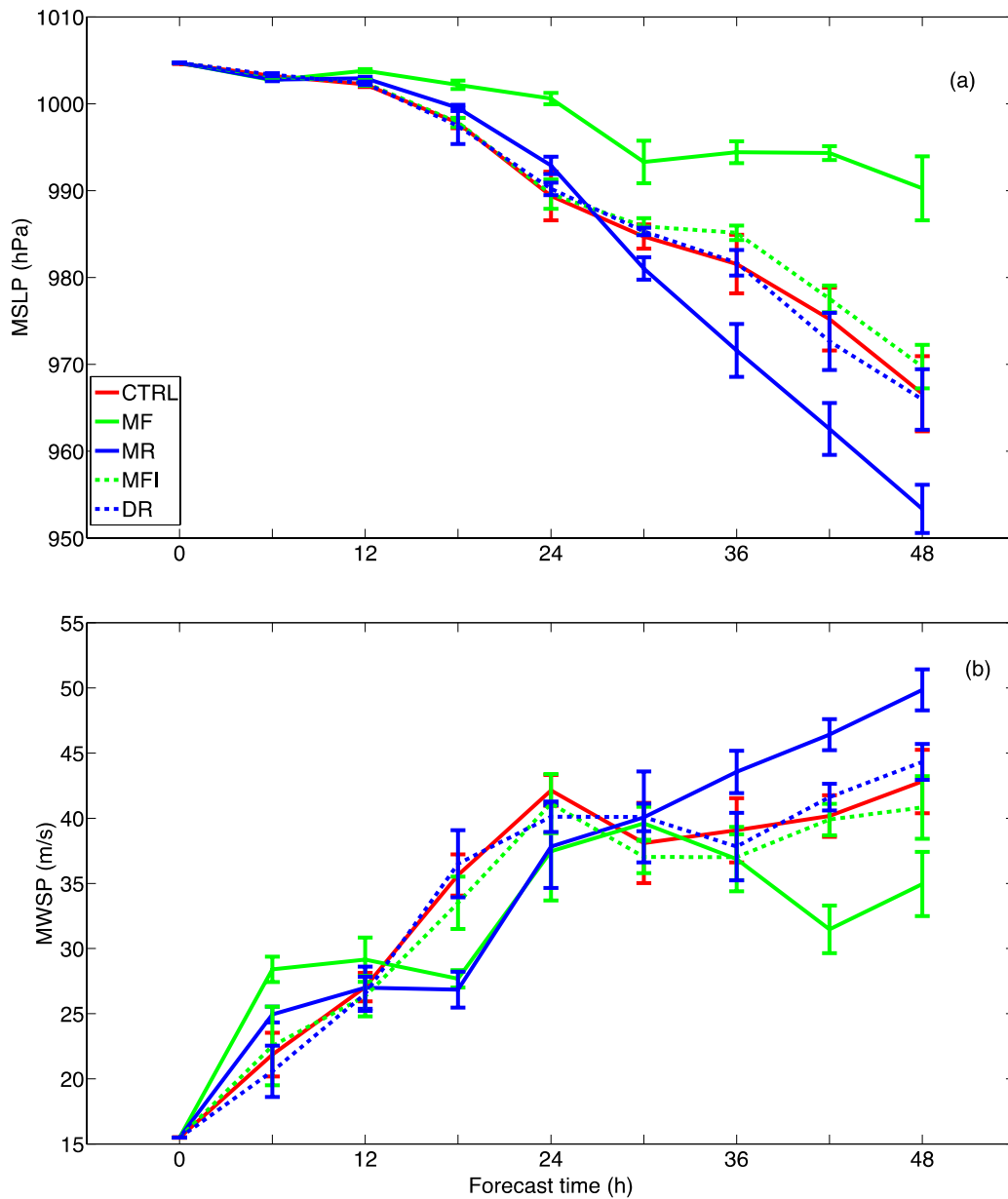
- 450 Wang, Z., M. T. Montgomery, C. Fritz, 2012(a): A First Look at the Structure of the Wave Pouch  
451 during the 2009 PREDICT–GRIP Dry Runs over the Atlantic. *Mon. Wea. Rev.*, 140, 1144–  
452 1163. doi: <http://dx.doi.org/10.1175/MWR-D-10-05063.1>
- 453 Wang, Z., T. J. Dunkerton, M. T. Montgomery, 2012(b): Application of the Marsupial Paradigm  
454 to Tropical Cyclone Formation from Northwestward-Propagating Disturbances. *Mon. Wea.*  
455 *Rev.*, 140, 66–76. doi: <http://dx.doi.org/10.1175/2011MWR3604.1>
- 456 Wu, L., H. Su, R. G. Fovell, B. Wang, J. T. Shen, B. H. Kahn, S. M. Hristova-Veleva, B. H.  
457 Lambriksen, E. J. Fetzer, and J. H. Jiang, 2012: Relationship of environmental relative  
458 humidity with North Atlantic tropical cyclone intensity and intensification rate, *Geophys. Res.*  
459 *Lett.*, 39, L20809, doi:10.1029/2012GL053546.
- 460 Ying, Y. and Q. Zhang, 2012: A Modeling Study on Tropical Cyclone Structural Changes in  
461 Response to Ambient Moisture Variations. *Journal of the Meteorological Society of Japan*,  
462 90(5), 755-770. Doi:10.2151/jmsj.2012-512
- 463

464 **List of Figures**

465

466 Figure 1. Column-integrated PWV (cm) at the initialization of the WRF simulations: (a) CTRL;

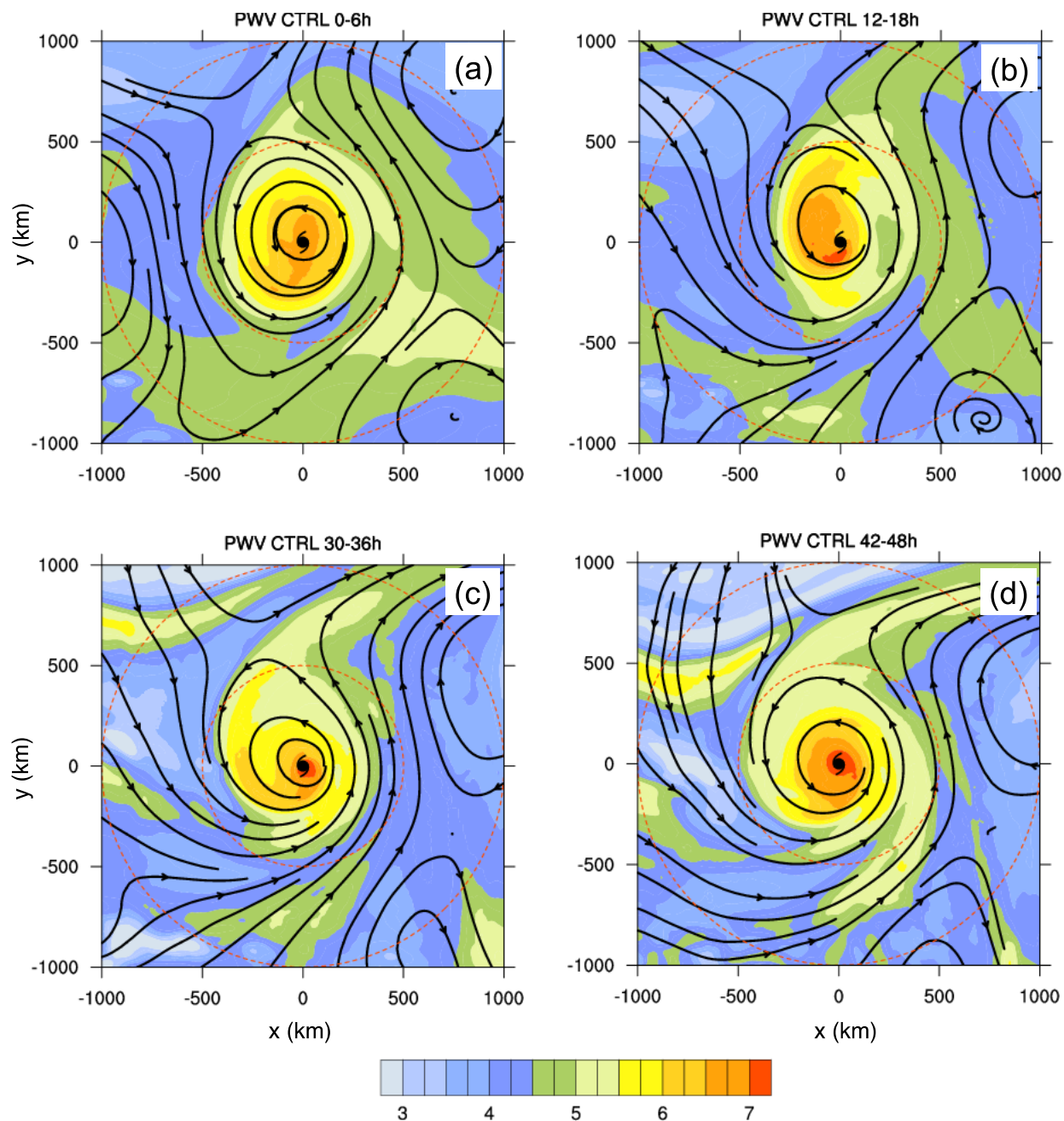
467 (b) MF; (c) MFI; (d) MR; (e) DR.



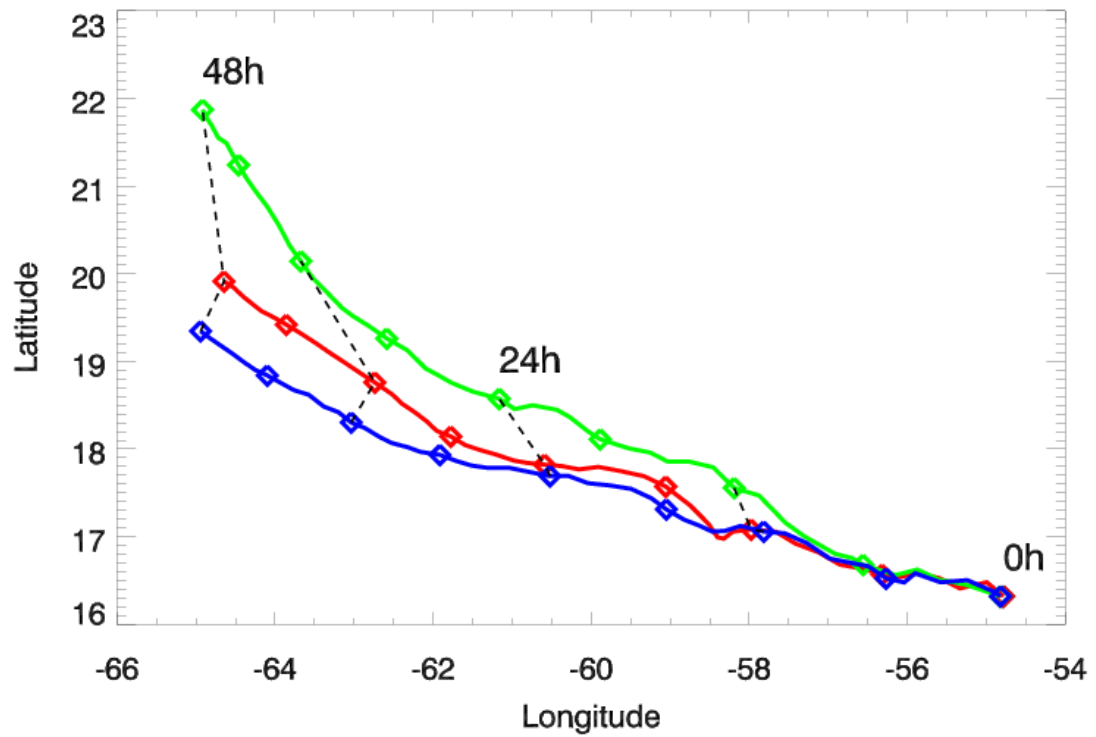
468

469 Figure 2. Time series of the model simulated ensemble mean and standard deviation of (a) MSLP

470 (hPa) and (b) MWSP ( $\text{m s}^{-1}$ ).



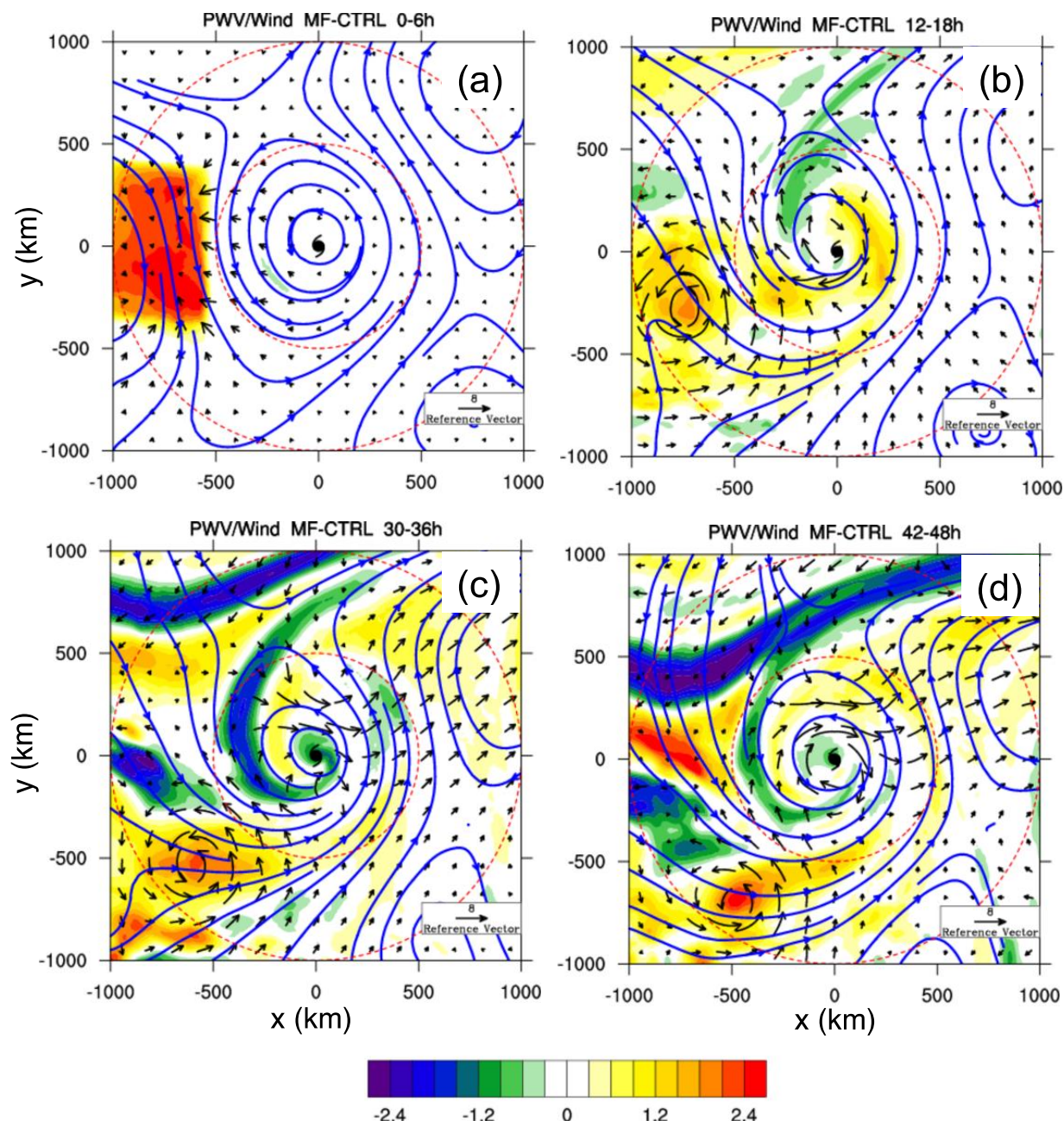
471  
 472 Figure 3. The mean translated streamline below 5 km and column-integrated PWV (cm)  
 473 (shading) in the WRF CTRL simulation in the storm following coordinate: (a) 0-6 h; (b) 12-18 h;  
 474 (c) 30-36 h; (d) 42-48 h. The hurricane symbol shows the TC center. The dashed red circles  
 475 represent the radius of 500 km and 1000 km, respectively. All the data are taken from the outer  
 476 model domain.



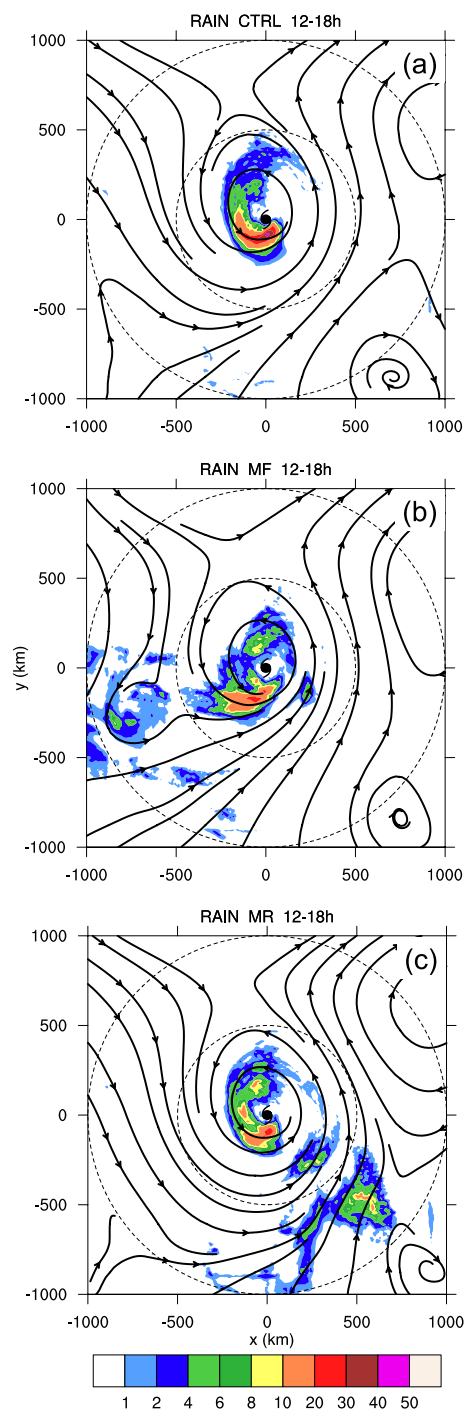
477

478 Figure 4. Storm tracks for CTRL (red), MF (green) and MR (blue). Every 6 h is identified with a  
 479 diamond symbol. Black dashed lines connect storm position at the same forecast time for every  
 480 12 h.



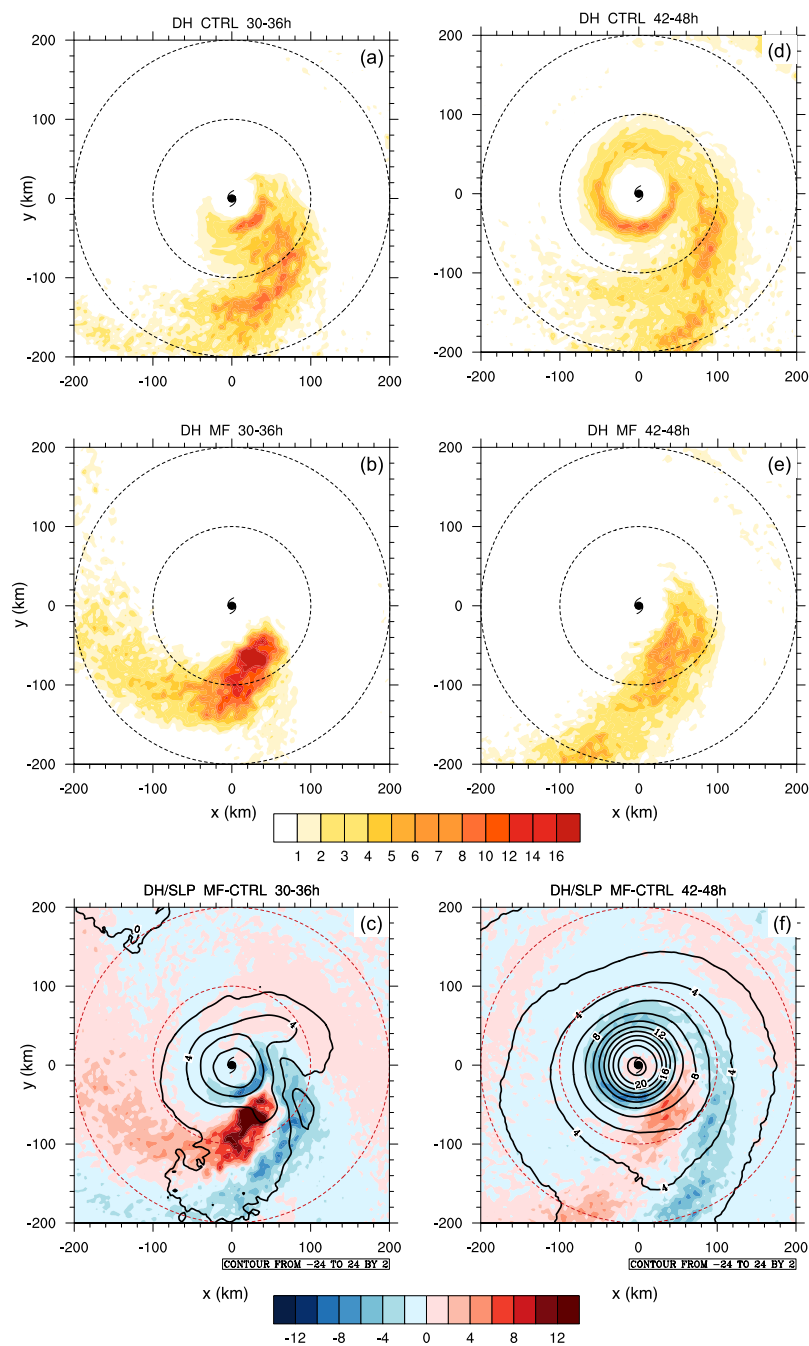


481  
 482 Figure 5. Differences of mean wind vector ( $\text{m s}^{-1}$ ) below 5 km and column-integrated PWV (cm)  
 483 (shading) between the MF and CTRL simulations in the storm following coordinate: (a) 0-6 h;  
 484 (b) 12-18 h; (c) 30-36 h; (d) 42-48 h. The blue streamline is the translated streamline at the co-  
 485 moving coordinate for the CTRL experiment at the corresponding time. The hurricane symbol  
 486 shows the TC center. The dashed red circles represent the radius of 500 km and 1000 km,  
 487 respectively. All the data are taken from the outer model domain. Mean wind vectors and  
 488 column-integrated PWV for CTRL and MF at each time are shown in supplementary Figure 1.



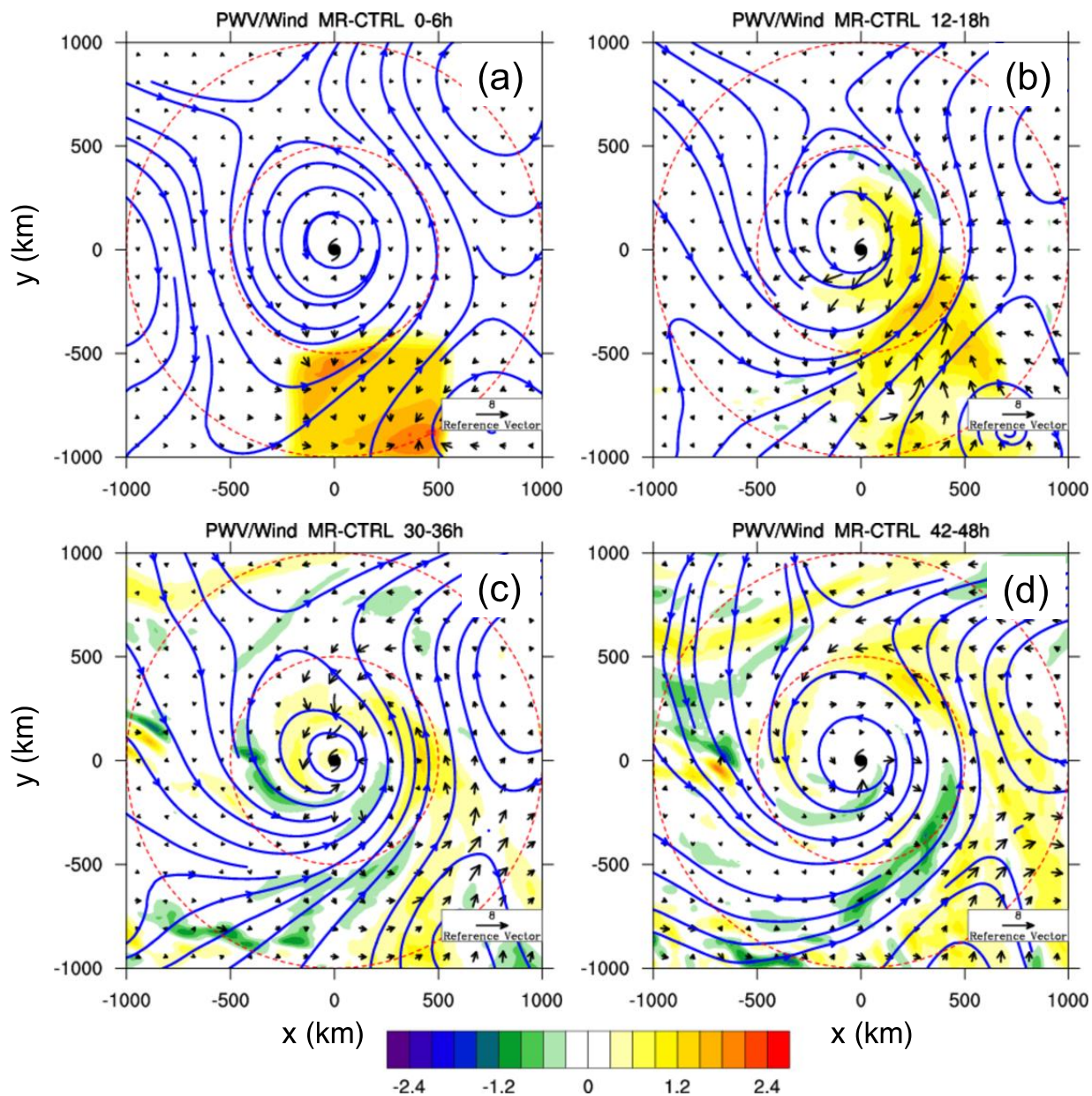
489

490 Figure 6. Mean rain rate ( $\text{mm hr}^{-1}$ ) and streamlines below 5 km during 12-18 h in the storm  
 491 following coordinate: (a) CTRL; (b) MF; (c) MR. The hurricane symbol shows the TC center.  
 492 The dashed black circles represent the radius of 500 km and 1000 km, respectively. All the data  
 493 are taken from the outer model domain.

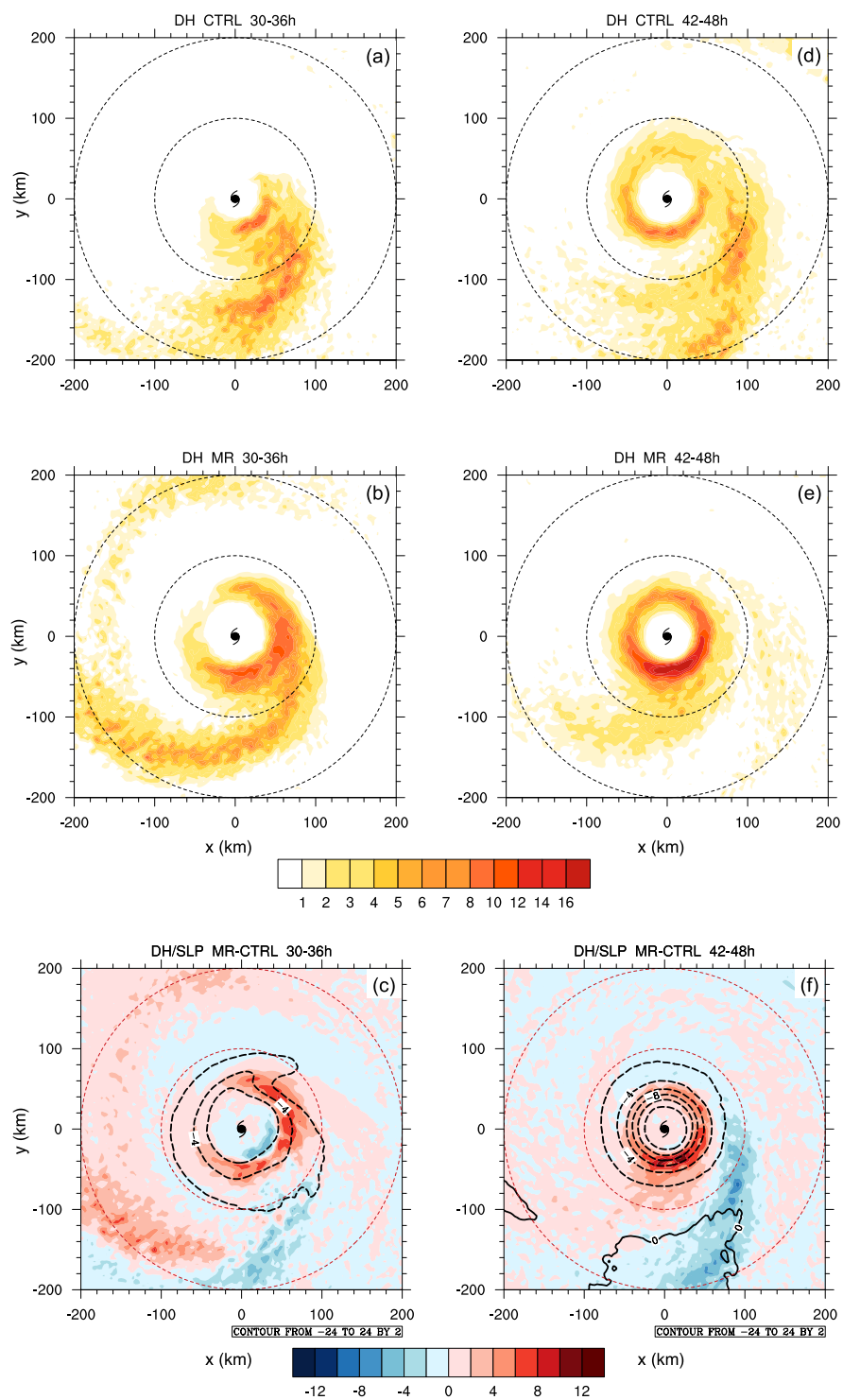


494

495 Figure 7. (a) Diabatic Heating (DH; K day<sup>-1</sup>) of CTRL in 30-36 h; (b) DH of MF in 30-36 h; (c)  
 496 the difference of DH and SLP between MF and CTRL in 30-36 h; (d) DH of CTRL in 42-48 h;  
 497 (e) DH of MF in 42-48 h; (f) the difference of DH and SLP between MF and CTRL in 42-48 h in  
 498 the storm following coordinate. The hurricane symbol shows the TC center. The dashed red  
 499 circles represent the radius of 100 km and 200 km, respectively. All the data are taken from the  
 500 inner model domain.

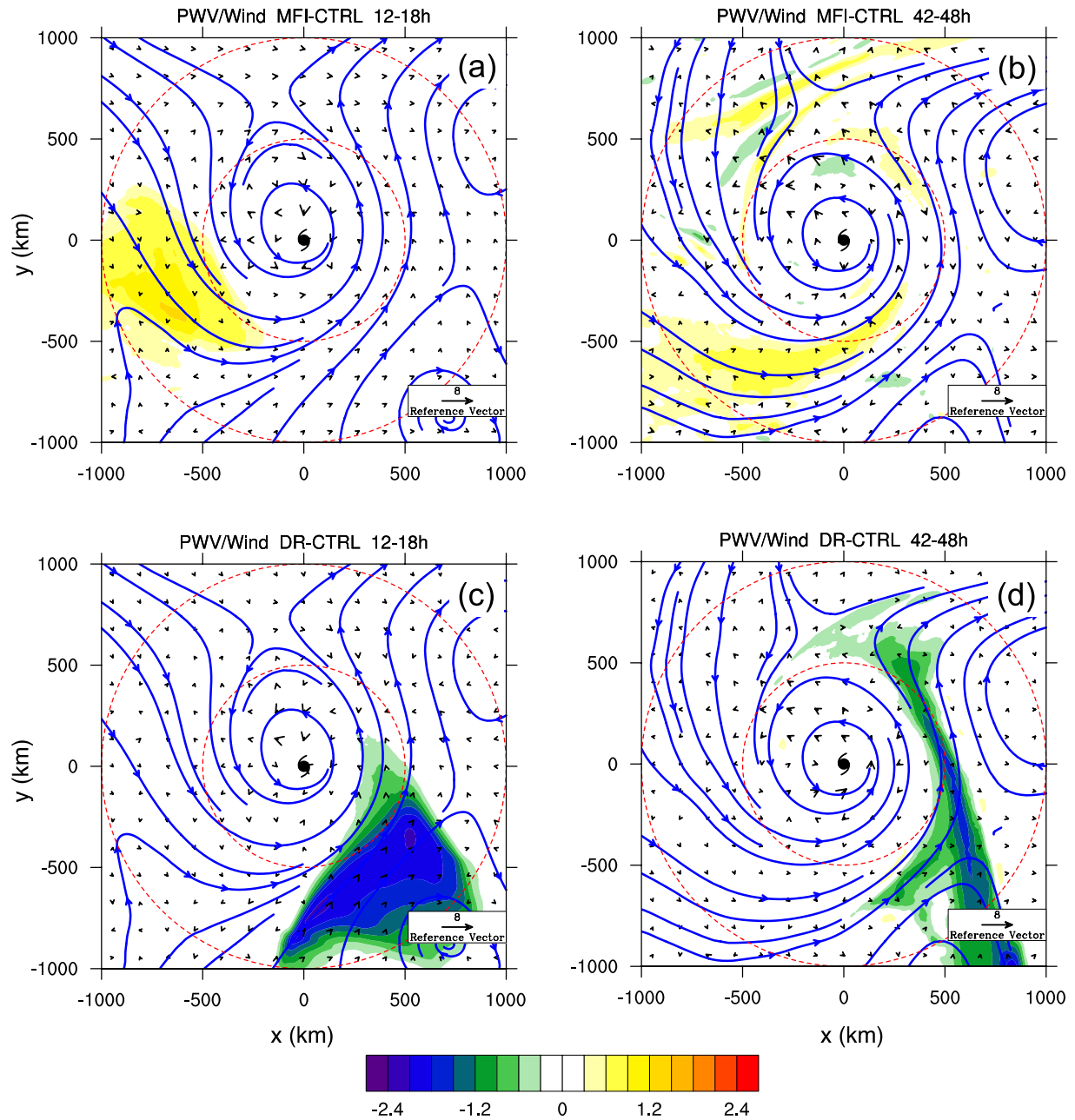


501  
 502 Figure 8. Same as Fig. 5, but for differences between the MR and CTRL experiments. Mean  
 503 wind vectors and column-integrated PWV for CTRL and MR at each time are shown in  
 504 supplementary Figure 1.



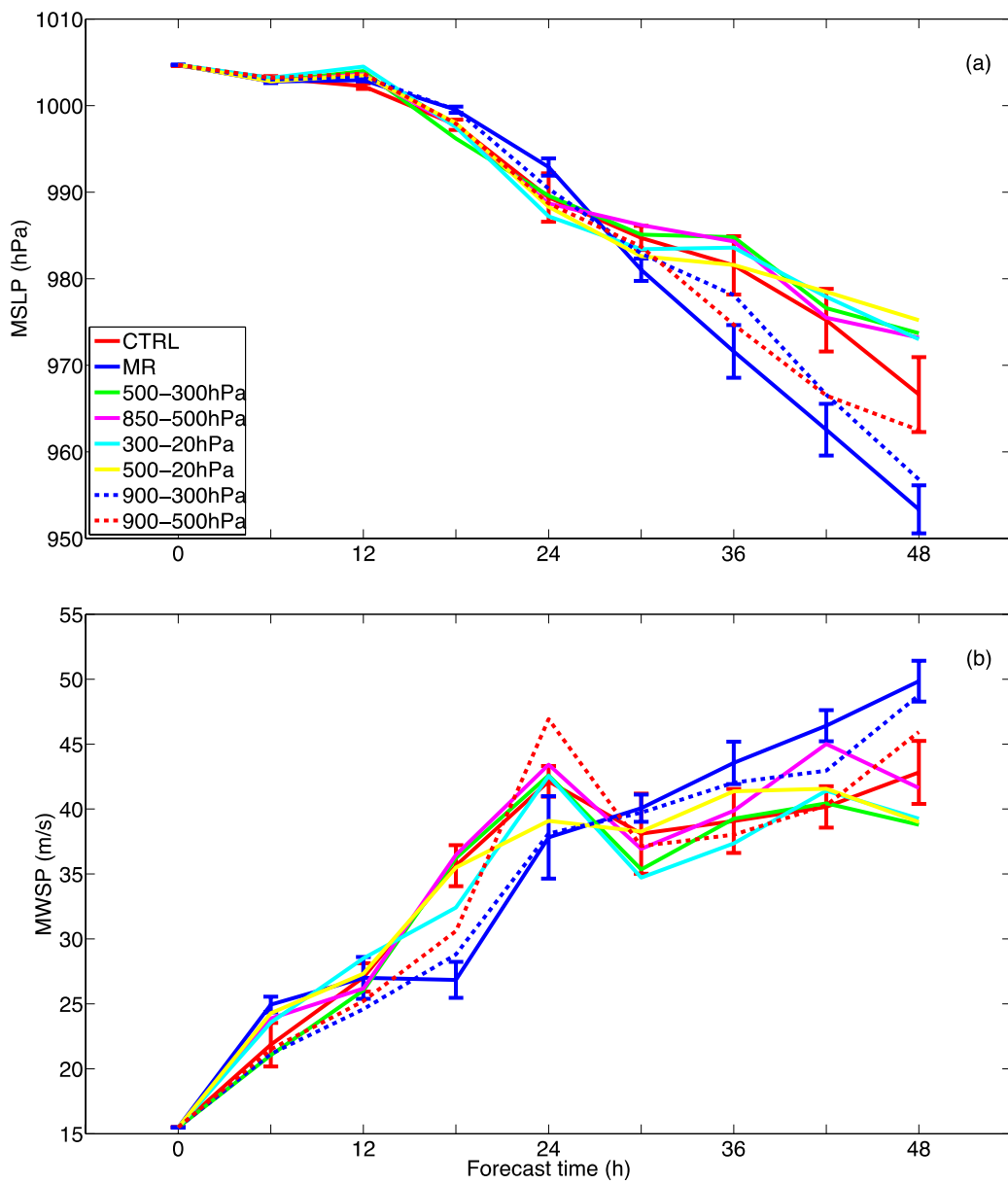
505

506 Figure 9. Same as Fig. 7 but for the MR and CTRL experiments.



507

508 Figure 10. Difference of mean wind vector below 5 km and column-integrated PWV (cm) in the  
 509 storm following coordinate: (a) MFI-CTRL for 12-18 h; (b) MFI-CTRL for 42-48 h; (c) DR-  
 510 CTRL for 12-18 h; (d) DR-CTRL for 42-48 h. The blue streamline is the translated streamline at  
 511 the co-moving coordinate for the CTRL case at corresponding time. The hurricane symbol shows  
 512 the TC center. The dashed red circles represent the radius of 500 km and 1000 km, respectively.  
 513 All the data are taken from the outer model domain.



514

515 Figure 11. Time series of the model simulated (a) MSLP (hPa) and (b) MWSP ( $\text{m s}^{-1}$ ). CTRL in  
 516 red; MR in blue; other simulations are same as the MR run, but with modification of moisture in  
 517 differently prescribed pressure layer.

518